Pergamon

Bioorganic & Medicinal Chemistry, Vol. 4, No. 12, pp 2091–2104, 1996

PII: S0968-0896(96)00220-9
0968-0896/96 $15.00+0.00

Structure–Activity Relationships of 2-Aryl-2,5-dihydropyridazino[4,3-*b*]indol-3(3H)-ones at the Benzodiazepine Receptor

F. Palluotto,[a] A. Carotti,[a] G. Casini,[a] F. Campagna,[a,*] G. Genchi,[b] M. Rizzo,[c] and G. B. De Sarro[d]

[a]*Dipartimento Farmacochimico and* [b]*Dipartimento Farmacobiologico, Università di Bari, via E. Orabona 4, I-70125 Bari, Italy*

[c]*Facoltà di Farmacia and* [d]*Dipartimento di Medicina Sperimentale e Clinica, Università di Reggio Calabria, via T.Campanella 88100-Catanzaro, Italy*

Abstract—A large series of 2-aryl-2,5-dihydropyridazino[4,3-b]indol-3(3H)ones (PIs) carrying properly selected substituents at the indole and N_2-phenyl rings was prepared and tested as central benzodiazepine receptor (BZR) ligands and potential (anti)convulsant agents. Stereoelectronic requirements for high receptor affinity were detected by means of 2-D and 3-D QSAR analyses. BZR affinities and pharmacological profiles of the compounds were examined in comparison with some other pyridazinoindolones recently described by us and with pyrazoloquinoline (PQ) analogues. An anticonvulsant activity greater than PQs was generally observed for PIs. Notably, in the test of audiogenically induced seizures, one compound showed a potency comparable to that of diazepam. Copyright © 1996 Elsevier Science Ltd

Introduction

Benzodiazepine receptor (BZR) ligands produce their pharmacological effects by modulating the action of GABA at the $GABA_A$-receptor/Cl^- ionophore supramolecular complex.[1,2] This complex can be formed by different combinations of distinct subunits called α, β, γ, δ, and ρ.[3,4] A pentameric model of the ligand-gated ion complex has been proposed.[5] BZR ligands bind at allosteric modulatory sites (ω sites) enhancing (agonists) or reducing (inverse agonists) the GABA-induced Cl^- ion flux. A third class of ligands, called antagonists, exhibit, per se, no relevant biological effects but antagonize the action of agonists and inverse agonists.[6] Ligand agonists such as the classical benzodiazepines are currently used in the treatment of anxiety and depressive disorders whereas antagonists, such as flumazenil, may be used to reverse the action of an overdose of benzodiazepine both in acute intoxication and in the induction of anaesthesia in surgical interventions. Despite the substantial advances in the knowledge of molecular pharmacology of anxiolitic drugs and the physiopathology of anxiety disorders, much remains to be achieved for the development of new and truly innovative drugs lacking the numerous side effects of benzodiazepines.[7]

In order to gain insight into the structure and function of the BZR, in the last decade many efforts have been made to detect the essential common structural features of the diverse classes of BZR ligands with varying affinities and intrinsic activities.[8–13]

In this context our interest has been recently focused on the synthesis, BZR binding and preliminary pharmacological characterization of a new class of BZR ligands, namely the 2-aryl-2,5-dihydropyridazino-[4,3-*b*]indol-3(3H)-ones (PIs).[14] Some PIs have shown an interesting anticonvulsant activity in both sound and pentylenetetrazole (PTZ) induced seizures in mice and very interestingly, a comparison of their receptor binding affinities, GABA ratios and pharmacological activities with those of pyrazoloquinoline analogues (PQs), a well known class of high affinity BZR ligands, had evidenced some distinct biochemical and pharmacological behaviour.[14]

In an attempt better to identify primary ligand–receptor interactions, and to define and improve the pharmacological profiles of PIs, a large series of them were prepared. In particular, the new compounds were designed to assess the importance of the indolic NH function as a hydrogen bond donor group and to explore the influence on the binding affinity of the hydrophobic, electronic and steric effects of the substituents at the indole and the N_2-phenyl rings.

To reach this goal, a classical QSAR (Hansch approach) and Comparative Molecular Field Analysis (CoMFA) were employed in the current study.

Results and Discussion

Chemistry

Scheme 1 outlines the synthetic route to PIs **6** and **7**. Some slight modifications of the procedures previously

reported by us[14] were made. In short, the isatins **1a–d** were refluxed with phosphorus pentachloride in anhydrous benzene to give the corresponding 2-chloro-3H-indol-3-ones (**2a–d**), which due to their ease of hydrolysis were used for the subsequent reaction without further purification. Treatment of **2a–d** with diethylmalonate sodium salt led to the corresponding 2-biscarbethoxymethylene-indolin-3-ones (**3a–d**), which were condensed with the appropriately substituted phenylhydrazine hydrochlorides to afford the pyridazinoindolone esters **4**. The esters **4** were hydrolized to the corresponding carboxylic acids **5**, which decarboxylated by heating to yield pyridazinoindolones **6**. By treating compounds **6e**, **h**, **j**, and **n** with sodium hydride and methyl iodide, the (N-5) methylated compounds **7e**, **h**, **j**, and **n** were obtained. The assignment of the methyl group at the *N*-5 position was based on the observation that the UV spectra did not differ significantly from those of the corresponding parent compounds **6e**, **h**, **j**, and **n** (Table 1). Moreover, physical and spectroscopic literature data of compounds **7e**, **h**, and **n**, already prepared by others[15] through a different and more difficult pathway, were fully consistent with those obtained by us. Physical and spectroscopic data of compounds **3–7** are listed in Table 2.

Binding studies

All the new ligands **6f**, **g**, **i–m**, **o–ω**, **7e**, **h**, **j**, and **n** were evaluated for their in vitro affinities at the BZR (Table 3) by the method previously described.[14] As can be inferred from the data showed in Table 3 for the reference PQ compounds (CGS 8216, 9895, and 9896), that method, partly changed from the classical one due to solubility problems of most PIs, led to IC_{50} values 4–10 times higher than those reported in the literature. This must be taken into account for a correct comparison with the binding data of other BZR ligands.

Our previous molecular modelling study[14] had shown that the lower BZR affinity of PIs **6** with respect to corresponding PQ analogues might result from the different distances between putative pharmacophoric elements. In particular, it may result from the impossibility to conserve at the same time an ideal geometry for the occurrence of two such energetically important interactions as π–π (or lipophilic) stacking in the L_1/L_2 pockets and the hydrogen bonding of the NH group, as outlined in the BZR pharmacophore model recently proposed by Cook.[13]

Data from the present work reveal that *para*-substitution at the N-2 phenyl ring enhances the receptor affinity more than *meta*- and *ortho*-substitutions. The loss of affinity in the *ortho*-substituted derivatives **6l** and **q** suggests severe steric contraints, in good agreement with previous findings.[13] The steric hindrance of the *ortho*-substituents at the inaccessible S_1 receptor region most likely induces a large out-of-plane twist of the N-2-phenyl ring which could be detrimental for an efficient π–π (or lipophilic) interaction.

Substitution at the indole aromatic ring with bromine at position 9 (**6w**) increases BZR binding with respect to the unsubstituted congener **6e**, while substitution at position 7 (**6u**) determines a dramatic reduction in BZR affinity. In contrast, substitution at position 8 (**6v**) does not alter the affinity for BZR. Interestingly, only in the case of **6v** the GABA ratio shifts towards a value much lower than 1 (0.78), which is characteristic of an inverse agonist activity.

Our findings with **6v** do not agree with the hypothesis of Fryer,[16] who suggested that substitution at position 8 in PQs may be considered equivalent to that of *para* position at the N2-phenyl ring allowing for two 'equivalent' binding modes resulting from a different ligand orientation inside the receptor active site. The prevalence of one orientation over the other could be determined by the relative lipophilicity of the benzene ring in the indole nucleus and of the N2-phenyl ring.

The *N*-methyl derivatives (**7e**, **h**, **j**, and **n**) exhibited very poor BZR affinity in contrast to the corresponding

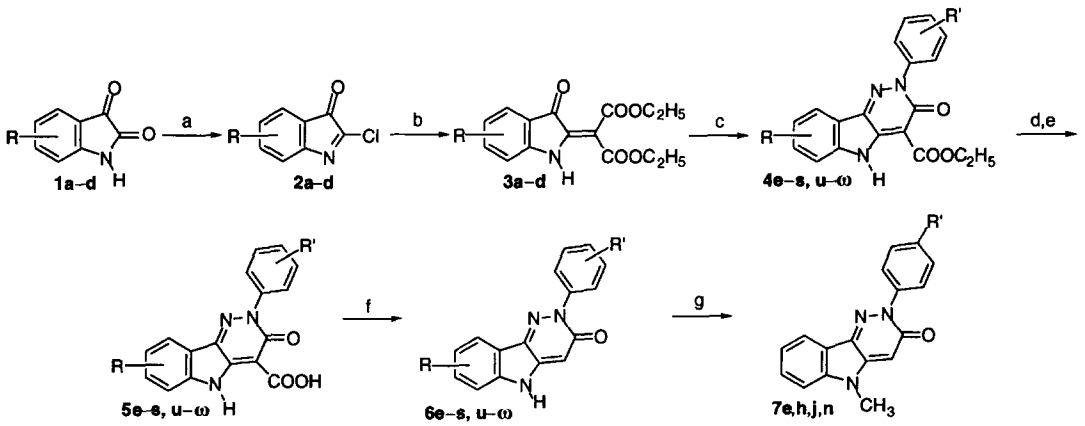

Scheme 1. **a**: R = H; **b**: R = Br (b_4:4-br; b_5:5-Br; b_6:6-Br; b_7 = 7-Br); **c**: R = 5-F; **d**: R = 5-CH_3; **e–s**: R = H; R′ = H (**e**), 4′-F (**f**), 3′-F (**g**), 4′-Cl (**h**), 3′-Cl (**i**), 4′-Br (**j**), 3′-Br (**k**), 2′-Br (**l**), 4′-I (**m**), 4′-OCH_3 (**n**), 4′-CH_3 (**o**), 3′-CH_3 (**p**), 2′-CH_3 (**q**), 4′-$CH(CH_3)_2$ (**r**), 4′-NO_2 (**s**); **u-y**: R′ = H; R = 7-Br (**u**), 8-Br (**v**), 9-Br (**w**), 8-CH_3 (**x**), 8-F (**y**); **z**: R = 8-CH_3; R′ = 4′-CH_3; **ω**: R = 8-F; R′ = 4-F. **6t**: R′ = -NH_2, R = H (see Experimental). Reagents. (a) PCl_5, anhydrous benzene, reflux; (b) $(COOC_2H_5)_2CH^-Na^+$, anhydrous dioxane, rt; (c) R′-$C_6H_4NHNH_2$·HCl, EtOH/H_2O, reflux; (d) NaOH, EtOH, reflux; (e) H^+, rt; (f) Δ, 320–360 °C; (g) NaH/anhydrous THF, CH_3I, rt.

Table 1. UV data (ethanol) of compounds **6e**, **h**, **j**, **n** and **7e**, **h**, **j**, **n**

Compound	λ_{max}, nm (log ε)		
6e	218 (4.43)	272 (4.60)	332 (3.77)
6h	220 (4.52)	272 (4.67)	332 (3.92)
6j	220 (4.51)	272 (4.66)	332 (3.92)
6n	218 (4.52)	268 (4.62)	338 (3.86)
7e	220 (4.51)	276 (4.68)	334 (3.85)
7h	222 (4.51)	276 (4.64)	334 (3.91)
7j	222 (4.44)	274 (4.58)	334 (3.84)
7n	222 (4.50)	270 (4.59)	340 (3.85)

non methylated compounds **6**. This dramatic drop in activity can be attributed to the steric hindrance of the methyl substituent and/or to the removal of a possible HB donation from the NH group to a proton-accepting group in the receptor.

2-D and 3-D QSAR studies

To obtain further valuable indications on the key structural elements that can modulate the BZR binding affinity of PIs **6** and **7**, we carried out quantitative structure–activity relationship studies using both the traditional Hansch approach[17] and the CoMFA.[18]

CoMFA is a relatively new 3-D QSAR methodology that is based on the assumption that the interaction between a ligand and its biological target is primarily non-covalent and shape-dependent. By sampling the steric and electrostatic fields surrounding a set of properly aligned ligands and correlating the energy changes with the biological activity (or any other target property) a 3-D QSAR model[19] can be derived.

2-D QSAR study (Hansch approach)

A multiple regression analysis (MRA) was performed on the binding data and chemical descriptors listed in Table 4. The electronic and hydrophobic effects of substituents were assessed by the classical Hammett and Hansch substituent constants, σ and π, respectively, whereas the molar refractivity MR and the STERIMOL Verloop parameters L, B_1, and B_5 were employed to model bulkiness and polarizability effects.[20]

In a first step, the MRA was carried out on the *para*-substituted congeners and the following equation was formulated:

$$pIC_{50} = 2.75\ (\pm 1.83)\ MR - 1.87\ (\pm 1.10)\ MR^2 + 6.43\ (\pm 0.53) \quad (1)$$

$$n = 10,\ r^2 = 0.708,\ s = 0.317,\ MR_0 = 0.735,$$

where n is the number of compounds, r is the correlation coefficient, s the standard deviation, MR is the molar refractivity and MR_0 is the optimal value of MR yielding a maximum pIC_{50} value.

In eq (1) the amino congener was a strong, and at the moment unexplainable, outlier; its dropping from the correlation led to eq (2) that presents much improved statistics:

$$pIC_{50} = 3.00\ (\pm 1.37)\ MR - 2.07\ (\pm 0.84)\ MR^2 + 6.46\ (\pm 0.49) \quad (2)$$

$$n = 9,\ r^2 = 0.866,\ s = 0.227,\ MR_0 = 0.725.$$

The above parabolic relationships indicated an ideal value of MR around 0.73 for maximum affinity. Since MR, by definition, encodes information both on the bulkiness and polarizability of a substituent, it is hard to get a definite indication as to the nature of the physico-chemical interactions involved in the ligand-receptor binding. However, we might hypothesize that the lipophilic receptor pocket named L_2 by Cook, has a limited accessibility and probably not a pure lipophilic character, but, as suggested by the presence of MR in eqs (1–2), should have a polar (or semipolar) nature, as observed in the past in several studies combining QSAR and modelling techniques.[21–24] No, or less significant, correlations were found with electronic or hydrophobic parameters.

In a second step, the QSAR study was extended to the *meta*-substituted congeners and to the N5-methyl substituted derivatives. The more heterogeneous character of the mixed sets was taken into account by using two indicator variables I_m and I_N that assume the values of 1 in the case of *meta* and N—CH_3 substituted congeners and zero in the other cases. For the whole set of compounds the following equation was derived:

$$pIC_{50} = 2.11\ (\pm 1.81)MR_4 - 1.54\ (\pm 1.25)MR^2_4 - 1.68\ (\pm 0.62)I_N + 6.58\ (\pm 0.51) \quad (3)$$

$$n = 18,\ r^2 = 0.715,\ s = 0.487,\ MR_0 = 0.69,$$

where MR_4 is the molar refractivity of the para substituents. The detrimental effect of the methylation at N5 is clearly pointed out by the strong negative coefficient with I_N in eq (3). The introduction into eq (3) of the second indicator variable I_m produced no statistical improvement.

Despite the useful indications given by eqs (1–3), the traditional QSAR approach has revealed its limitations in dealing with non-homologous series that were pooled together only by the use of indicator variables. To overcome this problem, the same set of BZR ligands were subjected to a 3-D QSAR study, based on the use of the CoMFA approach.[18] It has to be kept in mind that CoMFA results are largely dependent on the criteria used for molecular superimposition (alignment rules), which therefore constitute the most important and critical step in any CoMFA study. Fortunately, our set of compounds present no particular difficulty for molecular overlay since they have a common molecular skeleton, the tricyclic pyridazinoindole ring system, which was used as the template for fitting the whole set of ligands. The conformers selected upon a conformational analysis, carried out by a systematic search on the inter-ring torsion angle $C_3N_2C_1'C_2'$, had an equal torsion angle of −74° corresponding to a mean value for minimum energy conformers of *ortho* substituted congeners. For the *meta* and *para* substituted congeners that torsion angle corresponds to conformers very close to the absolute minimum (up to 1 kcal/mol).

Table 2. Physical and spectroscopical data of compounds **3–7**[a]

Compound	mp °C crystallization solvent	IR ν_{max}, cm^{-1}	^1H NMR[b] δ (ppm, *J* [Hz])
3b$_4$	134–136 (cyclohexane)	3360, 1720, 1695, 1685, 1600	1.30 (t, 3H, CH_3, *J* = 7.2); 1.35 (t, 3H, CH_3, *J* = 7.2); 4.27 (q, 2H, CH_2, *J* = 7.2); 4.40 (q, 2H, CH_2, *J* = 7.2); 6.85 (d, 1H, Arom, *J* = 7.7); 7.10 (d, 1H, Arom, *J* = 7.7); 7.20–7.40 (m, 1H, Arom); 9.20 (s, 1H, NH)
3b$_5$	145–147 (cyclohexane)	3350, 1745, 1685, 1610	1.31 (t, 3H, CH_3, *J* = 7.1); 1.36 (t, 3H, CH_3, *J* = 7.1); 4.29 (q, 2H, CH_2, *J* = 7.1); 4.40 (q, 2H, CH_2, *J* = 7.1); 6.80–6.90 (m, 1H, Arom); 7.55–7.65 (m, 1H, Arom); 7.70–7.80 (m, 1H, Arom); 9.19 (s, 1H, NH)
3b$_6$	159–162 (cyclohexane)	3290, 1730, 1675, 1600	1.30 (t, 3H, CH_3, *J* = 7.2); 1.35 (t, 3H, CH_3, *J* = 7.2); 4.28 (q, 2H, CH_2, *J* = 7.2); 4.39 (q, 2H, CH_2, *J* = 7.2); 7.05–7.15 (m, 2H, Arom); 7.45–7.50 (m, 1H, Arom); 9.18 (s, 1H, NH)
3c	118–120 (cyclohexane)	3370, 1730, 1680, 1610	1.31(t, 3H, CH_3, *J* = 7.2); 1.36(t, 3H, CH_3, *J* = 7.2); 4.27(q, 2H, CH_2, *J* = 7.2); 4.39(q, 2H, CH_2, *J* = 7.2); 6.80–6.90(m, 1H, Arom); 7.15–7.25(m, 1H, Arom); 7.25–7.35(m, 1H, Arom); 9.11(s, 1H, NH)
3d	166–168 (cyclohexane)	3320, 1710, 1680, 1620	1.30 (t, 3H, CH_3, *J* = 7.1); 1.35 (t, 3H, CH_3, *J* = 7.1); 2.29 (s, 3H, CH_3); 4.27 (q, 2H, CH_2, *J* = 7.1); 4.39 (q, 2H, CH_2, *J* = 7.1); 6.78 (d, 1H, Arom, *J* = 8.1); 7.25–7.35 (m, 1H, Arom); 7.40–7.45 (m, 1H, Arom); 9.05(s, 1H, NH).
4f	245–246 (ligroin)	3390, 1680, 1670, 1655, 1615	1.44 (t, 3H, CH_3, *J* = 7.1); 4.47 (q, 2H, CH_2, *J* = 7.1); 7.10–7.35 (m, 4H, Arom); 7.45–7.65 (m, 3H, Arom); 7.95–8.05 (m, 1H, Arom); 9.86 (s, 1H, NH)
4g	201–203 (acetonitrile)	3360, 1670, 1650, 1605	1.44 (t, 3H, CH_3, *J* = 7.2); 4.47 (q, 2H, CH_2, *J* = 7.2); 7.06–7.18 (m, 1H, Arom); 7.25–7.35 (m, 2H, Arom); 7.35–7.55 (m, 4H, Arom); 7.99 (d, 1H, Arom, *J* = 7.8); 9.86 (s, 1H, NH)
4i	193–195 (ligroin)	3390, 1680, 1660, 1610	1.44 (t, 3H, CH_3, *J* = 7.1); 4.47 (q, 2H, CH_2, *J* = 7.1); 7.25–7.35 (m, 2H, Arom); 7.35–7.45 (m, 2H, Arom); 7.45–7.60 (m, 2H, Arom); 7.60–7.70 (m, 1H, Arom); 7.95–8.05 (m, 1H, Arom); 9.85 (s, 1H, NH)
4k	246–248 (ligroin)	3360, 1675, 1605	1.44 (t, 3H, CH_3, *J* = 7.1); 4.47 (q, 2H, CH_2, *J* = 7.1); 7.20–7.40 (m, 3H, Arom); 7.45–7.65 (m, 3H, Arom); 7.80–7.85 (m, 1H, Arom); 7.95–8.05 (m, 1H, Arom); 9.85 (s, 1H, NH)
4l	200–202 (ligroin)	3330, 1670, 1640, 1605	1.43 (t, 3H, CH_3, *J* = 7.2); 4.45 (q, 2H, CH_2, *J* = 7.2); 7.20–7.40 (m, 3H, Arom); 7.45–7.55 (m, 3H, Arom); 7.73 (d, 1H, Arom, *J* = 8.1); 7.98 (d, 1H, Arom, *J* = 8.1); 9.91 (s, 1H, NH)
4m	263–264 (ligroin)	3365, 1675, 1650, 1610	1.43 (t, 3H, CH_3, *J* = 7.1); 4.46 (q, 2H, CH_2, *J* = 7.1); 7.25–7.35 (m, 2H, Arom); 7.35–7.45 (m, 2H, Arom); 7.45–7.55 (m, 1H, Arom); 7.75–7.85 (m, 2H, Arom); 7.90–8.00 (m, 1H, Arom); 9.87 (s, 1H, NH)
4o	255–257 (ligroin)	3380, 1680, 1670, 1655, 1615	1.44 (t, 3H, CH_3, *J* = 7.1); 2.41 (s, 3H, CH_3); 4.47 (q, 2H, CH_2, *J* = 7.1); 7.20–7.35 (m, 4H, Arom); 7.40–7.55 (m, 3H, Arom); 7.95–8.05 (m, 1H, Arom); 9.85 (s, 1H, NH)
4p	246–248 (ligroin)	3240, 1715, 1610	1.43 (t, 3H, CH_3, *J* = 7.1); 2.40 (s, 3H, CH_3); 4.46 (q, 2H, CH_2, *J* = 7.1); 7.20–7.32 (m, 3H, Arom); 7.35–7.45 (m, 3H, Arom); 7.45–7.55 (m, 1H, Arom); 7.99 (d, 1H, Arom, *J* = 8.0); 9.84 (s, 1H, NH).
4q	230–232 (ligroin)	3360, 1665, 1650, 1605	1.43 (t, 3H, CH_3, *J* = 7.1); 2.17 (s, 3H, CH_3); 4.45 (q, 2H, CH_2, *J* = 7.1); 7.20–7.40 (m, 6H, Arom); 7.45–7.55 (m, 1H, Arom); 7.97 (d, 1H, Arom, *J* = 7.7); 9.84 (s, 1H, NH)
4r	203–205 (ligroin)	3370, 1665, 1645, 1605	1.27 (d, 6H, $2CH_3$, *J* = 6.9); 1.43 (t, 3H, CH_3, *J* = 7.1); 2.96 (st, 1H, CH, *J* = 6.9); 4.51 (q, 2H, CH_2 *J* = 7.1); 7.20–7.35 (m, 4H, Arom); 7.45–7.55 (m, 3H, Arom); 7.98 (d, 1H, Arom, *J* = 7.1); 9.84 (s, 1H, NH)
4s	267– 269 (acetonitrile)	3400, 1690, 1665, 1615	1.46 (t, 3H, CH_3, *J* = 7.1); 4.50 (q, 2H, CH_2, *J* = 7.1); 7.25–7.35 (m, 2H, Arom); 7.50–7.60 (m, 1H, Arom); 7.85–8.05 (m, 3H, Arom); 8.25–8.40 (m, 2H, Arom); 9.89 (s, 1H, NH)
4u	258–259 (ligroin)	3220, 1675, 1640, 1600	1.43 (t, 3H, CH_3, *J* = 7.2); 4.46 (q, 2H, CH_2, *J* = 7.2); 7.35–7.55 (m, 5H, Arom); 7.55–7.65 (m, 2H, Arom); 7.83 (d, 1H, Arom, *J* = 8.2); 9.85 (s, 1H, NH)
4v	255–257 (ligroin)	3370, 1675, 1650, 1610	1.43 (t, 3H, CH_3, *J* = 7.1); 4.46 (q, 2H, CH_2, *J* = 7.1); 7.15–7.25 (m, 1H, Arom); 7.35–7.65 (m, 6H, Arom); 8.05–8.15 (m, 1H, Arom); 9.85 (s, 1H, NH)
4w	210–212 (ligroin)	3390, 1715, 1605	1.43 (t, 3H, CH_3, *J* = 7.1); 4.47(q, 2H, CH_2, *J* = 7.1); 7.20–7.55 (m, 6H, Arom); 7.65–7.75 (m, 2H, Arom); 9.93 (s, 1H, NH)
4x	214–216 (ligroin)	3345, 2910, 1670, 1640, 1610	1.43 (t, 3H, CH_3, *J* = 7.1); 2.43 (s, 3H, CH_3); 4.45 (q, 2H, CH_2, *J* = 7.1); 7.16 (d, 1H, Arom, *J* = 8.2); 7.25–7.35 (m, 1H, Arom); 7.35–7.55 (m, 3H, Arom); 7.55–7.70 (m, 2H, Arom); 7.79 (s, 1H, Arom); 9.75 (s, 1H, NH)
4y	235–237 (ligroin)	3360, 1670, 1640	1.43 (t, 3H, CH_3, *J* = 7.1); 4.46 (q, 2H, CH_2, *J* = 7.1); 7.15–7.30 (m, 2H, Arom); 7.35–7.55 (m, 3H, Arom); 7.55–7.65 (m, 2H, Arom); 7.65–7.75 (m, 1H, Arom); 9.82 (s, 1H, NH)

Table 2. Continued

Compound	mp °C crystallization solvent	IR ν_{max}, cm^{-1}	^1H NMR[b] δ (ppm, *J* [Hz])
4z	258–260 (ligroin)	3310, 1725, 1615, 1560	1.44 (t, 3H, CH_3, $J=7.1$); 2.41 (s, 3H, CH_3); 2.44 (s, 3H, CH_3); 4.46 (q, 2H, CH_2, $J=7.1$); 7.13–7.35 (m, 4H, Arom); 7.40–7.55 (m, 2H, Arom); 7.75–7.85 (m, 1H, Arom); 9.75(s, 1H, NH)
4ω	210–212 (ligroin)	3380, 1670, 1650	1.44 (t, 3H, CH_3, $J=7.1$); 4.47 (q, 2H, CH_2, $J=7.1$); 7.10–7.30 (m, 4H, Arom); 7.50–7.70 (m, 3H, Arom); 9.84 (s, 1H, NH)
5f	330–332 dec (AcOH)	3280, 1730, 1655, 1625	7.25–7.50 (m, 3H, Arom); 7.55–7.75 (m, 4H, Arom); 8.01 (d, 1H, Arom, $J=7.8$); 12.00–12.40 (br, 1H, NH); 14.20–14.60(br, 1H, COOH)
5g	321–324 (dioxane)	3260, 1710, 1640, 1595	7.30–7.45 (m, 2H, Arom); 7.50–7.70 (m, 5H, Arom); 8.03 (d, 1H, Arom, $J=7.6$); 12.20 (s, 1H, NH); 14.28 (s, 1H, COOH)
5i	320–322 (dioxane)	3280, 1715, 1640, 1610	7.30–7.40 (m, 1H, Arom); 7.55–7.70 (m, 5H, Arom); 7.75–7.85 (m, 1H, Arom); 8.03 (d, 1H, Arom, $J=7.3$); 12.10–12.30 (br, 1H, NH); 14.10–14.40 (br, 1H, COOH)
5k	319–322 (dioxane)	3280, 1710, 1640, 1610	7.30–7.40 (m, 1H, Arom); 7.50–7.80 (m, 5H, Arom); 7.90–7.95 (m, 1H, Arom); 8.03 (d, 1H, Arom, $J=7.9$); 12.10–12.40 (br, 1H, NH); 14.10–14.40 (br, 1H, COOH)
5l	318–320 (dioxane)	3300, 1705, 1640, 1610	7.30–7.40 (m, 1H, Arom); 7.50–7.60 (m, 1H, Arom); 7.60–7.70 (m, 3H, Arom); 7.70–7.75 (m, 1H, Arom); 7.85–7.95 (m, 1H, Arom); 8.03 (d, 1H, Arom, $J=7.5$); 12.29 (s, 1H, NH); 14.11(s, 1H, COOH)
5m	328–330 (dioxane)	3320, 1705, 1640, 1610	7.25–7.35 (m, 1H, Arom); 7.40–7.50 (m, 2H, Arom); 7.55–7.70 (m, 2H, Arom); 7.90–8.05 (m, 3H, Arom); 12.10–12.30 (br, 1H, NH); 14.20–14.40 (br, 1H, COOH)
5o	328–330 dec (AcOH)	3290, 1725, 1655, 1625	2.40 (s, 3H, CH_3); 7.25–7.70 (m, 7H, Arom); 8.00 (d, 1H, Arom, $J=7.7$); 12.00–12.30 (br, 1H, NH); 14.30–14.70 (br, 1H, COOH)
5p	319–322 (dioxane)	3440br, 3280br, 1720, 1640, 1610	2.40 (s, 3H, CH_3); 7.25–7.40 (m, 2H, Arom); 7.40–7.50 (m, 3H, Arom); 7.55–7.70 (m, 2H, Arom); 8.01 (d, 1H, Arom, $J=7.7$); 12.00–12.30 (br, 1H, NH)
5q	315–318 (dioxane)	3260, 1700, 1640, 1610	2.10 (s, 3H, CH_3); 7.30–7.40 (m, 1H, Arom); 7.40–7.55 (m, 4H, Arom); 7.55–7.70 (m, 2H, Arom); 8.01 (d, 1H, Arom, $J=7.6$); 12.22 (s, 1H, NH); 14.30–14.50 (br, 1H, COOH)
5r	315–318 (AcOH)	3320, 1700, 1640, 1605	1.25 (d, 6H, $2CH_3$, $J=6.9$); 3.00 (st, 1H, CH, $J=6.9$); 7.30–7.40 (m, 1H, Arom); 7.40–7.50 (m, 2H, Arom); 7.50–7.60 (m, 2H, Arom); 7.60–7.70 (m, 2H, Arom); 8.00 (d, 1H, Arom, $J=7.7$); 12.10–12.30 (br, 1H, NH)
5s	337–339 dec (AcOH)	3280, 1725, 1655, 1625	7.25–7.40 (m, 1H, Arom); 7.60–7.65 (m, 2H, Arom); 7.95–8.05 (m, 3H, Arom); 8.40–8.50 (m, 2H, Arom); 12.00–12.50 (br, 1H, NH); 13.80–14.40 (br, 1H, COOH)
5u	324–326 (dioxane)	3240, 1705, 1640, 1605	7.40–7.65 (m, 6H, Arom); 7.78 (d, 1H, Arom, $J=1.4$); 7.93 (d, 1H, Arom, $J=8.3$); 12.50–13.50 (br, 1H)
5v	>350 dec (AcOH)	3310, 1725, 1655, 1615	7.50–7.80 (m, 7H, Arom); 8.15–8.20 (m, 1H, Arom); 12.10–12.5 (br, 1H, NH); 14.10–14.50 (br, 1H, COOH)
5w	>350 (dioxane)	3240, 1720, 1710, 1640, 1605	7.45–7.70 (m, 8H, Arom); 12.25–12.45 (br, 1H, NH); 14.30–14.50 (br, 1H, COOH)
5x	325–328 (dioxane)	3310, 1710, 1640, 1620	2.40 (s, 3H, CH_3); 7.40–7.70 (m, 7H, Arom); 7.82 (s, 1H, Arom); 12.07 (s, 1H, NH); 14.45 (s, 1H, COOH)
5y	320–322 (AcOH)	3290, 1710, 1640, 1620	7.40–7.70 (m, 7H, Arom); 7.85–7.95 (m, 1H, Arom); 12.10–12.30 (br, 1H, NH); 14.20–14.50 (br, 1H, COOH)
5z	326–328 (AcOH)	3300, 1700, 1645, 1615	2.40 (s, 6H, $2CH_3$); 7.25–7.45 (m, 3H, Arom); 7.45–7.60 (m, 3H, Arom); 7.82 (s, 1H, Arom); 12.07 (s, 1H, NH); 14.51 (s, 1H, COOH)
5ω	>350 (AcOH)	3260, 1710, 1640	7.30–7.55 (m, 3H, Arom); 7.55–7.80 (m, 3H, Arom); 7.85–7.95 (m, 1H, Arom); 12.21 (s, 1H, NH); 14.29 (s, 1H, COOH)
6f	345–348.5 dec (dioxane)	3200, 1670, 1620, 1565	6.49 (s, 1H, CH-C—O); 7.10–7.25 (m, 1H, Arom); 7.30–7.40 (m, 3H, Arom); 7.50–7.55 (m, 1H, Arom); 7.60–7.70 (m, 2H, Arom); 7.89 (d, 1H, Arom, $J=7.4$); 11.22 (s, 1H, NH)

Table 2. Continued

Compound	mp °C crystallization solvent	IR ν_{max}, cm^{-1}	^1H NMR[b] δ (ppm, *J* [Hz])
6g	348–350 dec (dioxane)	3230, 1660, 1640, 1610, 1560	6.49 (s, 1H, CH-C—O); 7.10–7.25 (m, 1H, Arom); 7.25–7.40 (m, 2H, Arom); 7.45–7.60 (m, 4H, Arom); 7.91 (d, 1H, Arom, *J* = 7.6); 11.24 (s, 1H, NH)
6i	312–314 (dioxane)	3360, 1675, 1665, 1650, 1610, 1520	6.50 (s, 1H, CH-C—O); 7.15–7.25 (m, 1H, Arom); 7.32 (d, 1H, Arom, *J* = 8.0); 7.45–7.65 (m, 4H, Arom); 7.70–7.75 (m, 1H, Arom); 7.92 (d, 1H, Arom, *J* = 7.4); 10.70–10.90 (br, 1H, NH)
6k	317–319 (dioxane)	3120, 1660, 1610, 1460	6.50 (s, 1H, CH-C—O); 7.15–7.25 (m, 1H, Arom); 7.32 (d, 1H, Arom, *J* = 8.0); 7.45–7.60 (m, 2H, Arom); 7.60–7.70 (m, 2H, Arom); 7.85–7.90 (m, 1H, Arom); 7.92 (d, 1H, Arom, *J* = 7.5); 11.25 (s, 1H, NH)
6l	283–285 (dioxane)	3120, 1660, 1645, 1600, 1550	6.51 (s, 1H, CH-C—O); 7.10–7.20 (m, 1H, Arom); 7.33 (d, 1H, Arom, *J* = 8.0); 7.40–7.60 (m, 4H, Arom); 7.80–7.85 (m, 1H, Arom); 7.88 (d, 1H, Arom, *J* = 7.7); 11.27 (s, 1H, NH)
6m	335–337 (dioxane)	3100, 1660, 1640, 1600, 1545	6.48 (s, 1H, CH-C—O); 7.15–7.20 (m, 1H, Arom); 7.32 (d, 1H, Arom, *J* = 8.0); 7.40–7.55 (m, 3H, Arom); 7.85–7.95 (m, 3H, Arom); 11.10–11.30 (br, 1H, NH)
6o	317–322 dec (dioxane)	3160, 1670, 1650, 1615, 1555	2.37 (s, 3H, CH_3); 6.47 (s, 1H, CH-C—O); 7.10–7.20 (m, 1H, Arom); 7.25–7.35 (m, 3H, Arom); 7.40–7.55 (m, 3H, Arom); 7.88 (d, 1H, Arom, *J* = 7.5); 11.10–11.40 (br, 1H, NH)
6p	300–302 (dioxane)	3140, 1655, 1640, 1600, 1550	2.38 (s, 3H, CH_3); 6.48 (s, 1H, CH-C—O); 7.10–7.20 (m, 1H, Arom); 7.20–7.30 (m, 1H, Arom); 7.30–7.45 (m, 4H, Arom); 7.45–7.55 (m, 1H, Arom); 7.89 (d, 1H, Arom, *J* = 7.7); 11.25 (s, 1H, NH)
6q	298–300 (dioxane)	3120, 1660, 1640, 1600, 1550	2.04 (s, 3H, CH_3); 6.50 (s, 1H, CH-C—O); 7.10–7.20 (m, 1H, Arom); 7.30–7.45 (m, 5H, Arom); 7.45–7.55 (m, 1H, Arom); 7.87 (d, 1H, Arom, *J* = 8.0); 11.25 (s, 1H, NH)
6r	259–260 (AcOEt)	3150br, 1650, 1605, 1595, 1550	1.25 (d, 6H, $2CH_3$, *J* = 6.9); 2.97 (st, 1H, CH, *J* = 6.9); 6.47 (s, 1H, CH-C—O); 7.15–7.25 (m, 1H, Arom); 7.30–7.45 (m, 3H, Arom); 7.45–7.55 (m, 3H, Arom); 7.88 (d, 1H, Arom, *J* = 7.7); 11.20 (s, 1H, NH)
6s	320–322 dec (AcOEt)	3160, 1670, 1650, 1610, 1570	6.53 (s, 1H, CH-C—O); 7.15–7.25 (m, 1H, Arom); 7.33 (d, 1H, Arom, *J* = 8.1); 7.45–7.60 (m, 1H, Arom); 7.90–8.05 (m, 3H, Arom); 8.35–8.45 (m, 2H, Arom); 11.10–11.40 (br, 1H, NH)
6t	331–333 dec (acetonitrile)	3500, 3400, 3100 br, 1675, 1620, 1560	5.31 (s, 2H, NH_2); 6.42 (s, 1H, CH-C—O); 6.60–6.65 (m, 2H, Arom); 7.10–7.20 (m, 3H, Arom); 7.30 (d, 1H, Arom, *J* = 8.0); 7.45–7.55 (m, 1H, Arom); 7.86 (d, 1H, Arom, *J* = 7.4); 11.13 (s, 1H, NH)
6u	324–326 (dioxane)	3100, 1660, 1600	5.52 (s, 1H, CH-C—O); 6.10–6.15 (m, 1H, Arom); 6.15–6.35 (m, 6H, Arom); 6.48 (d, 1H, Arom, *J* = 6.1); 8.80–9.20 (br, 1H, NH)
6v	>350 (dioxane)	3180, 1675, 1655, 1625, 1560	6.53 (s, 1H, CH-C—O); 7.29 (d, 1H, Arom, *J* = 8.6); 7.40–7.70 (m, 6H, Arom); 8.00–8.05 (m, 1H, Arom); 11.10–11.40 (br, 1H, NH)
6w	>350 (dioxane)	3140, 1640, 1600	6.53 (s, 1H, CH); 7.30–7.45 (m, 4H, Arom); 7.45–7.60 (m, 2H, Arom); 7.60–7.70 (m, 2H, Arom); 11.00–11.50 (br, 1H, NH)
6x	345 dec (dioxane)	3100, 1655, 1605, 1550	2.37 (s, 3H, -CH_3); 6.44 (s, 1H, CH-C—O); 7.21 (d, 1H, Arom, *J* = 8.2); 7.25–7.35 (m, 1H, Arom); 7.35–7.65 (m, 5H, Arom); 7.70 (s, 1H, Arom); 11.08 (s, 1H, NH)
6y	349–350 (dioxane)	3110, 1660, 1610, 1550	6.50 (s, 1H, CH-C—O); 7.28–7.37 (m, 2H, Arom); 7.35–7.60 (m, 5H, Arom); 7.70–7.75 (m, 1H, Arom); 11.24 (s, 1H, NH)
6z	313–315 dec (dioxane)	3120, 1660, 1615, 1560	2.37 (s, 6H, $2CH_3$); 6.42 (s, 1H, CH-C—O); 7.20 (d, 1H, Arom, *J* = 8.2); 7.25–7.35 (m, 3H, Arom); 7.40–7.50 (m, 2H, Arom); 7.69 (s, 1H, Arom); 11.06 (s, 1H, NH)
6ω	>350 (dioxane)	3120, 1660, 1610, 1590, 1550	6.51 (s, 1H, CH-C—O); 7.25–7.45 (m, 4H, Arom); 7.55–7.65 (m, 2H, Arom); 7.65–7.75 (m, 1H, Arom); 11.24 (s, 1H, NH)
7e	217–219 (MeOH)	1650, 1620	3.60 (s, 3H, CH_3); 6.68 (s, 1H, CH-C—O); 7.15–7.30 (m, 1H, Arom); 7.40–7.65 (m, 7H, Arom); 7.91 (d, 1H, Arom, *J* = 7.7)
7h	273–274 (MeOH)	1655, 1620	3.60 (s, 3H, CH_3); 6.69 (s, 1H, CH-C—O);7.20–7.30 (m, 1H, Arom); 7.46 (d, 1H, Arom, *J* = 8.2); 7.55–7.70 (m, 5H, Arom); 7.92 (d, 1H, Arom, *J* = 7.6)
7j	272–274 (dioxane)	1660, 1625	3.60 (s, 3H, CH_3); 6.69 (s, 1H, CH-C—O); 7.15–7.30 (m, 1H, Arom); 7.45 (d, 1H, Arom, *J* = 8.1); 7.55–7.65 (m, 3H, Arom); 7.65–7.75 (m, 2H, Arom); 7.92 (d, 1H, Arom, *J* = 7.6)
7n	220–222 (MeOH)	1655, 1620	3.60 (s, 3H, CH_3); 3.81 (s, 3H, OCH_3); 6.66 (s, 1H, CH-C—O); 7.00–7.10 (m, 2H, Arom); 7.21 (t, 1H, Arom, *J* = 7.4); 7.40–7.55 (m, 3H, Arom); 7.55–7.65 (m, 1H, Arom); 7.91 (d, 1H, Arom, *J* = 7.6)

[a]Physical and spectroscopical data of compounds **3a** and **4**, **5**, **6e**, **h**, **j**, **n** were reported in our previous paper.[14]
[b]The ^1H NMR spectra were recorded in $CDCl_3$ (**3** and **4**) or in DMSO-d_6 (**5**, **6**, and **7**).

In the absence of any indication about the relative position of the *ortho* and *meta* substituents in binding to the BZR, two different alignments, leading to topologies A and B depicted in Table 5, were examined. For alignment A the *meta* substituents were considered at position 5′, whereas for alignment B they were at position 3′. Since the best statistical results were obtained from the molecules oriented according to alignment B, this alignment was retained to develop the final, non cross-validated, 3-D QSAR model. Both electrostatic and steric fields were necessary to get significant models; the contributions of the steric and electrostatic fields to the final model were 76 and 24%, respectively.

The final model based on the optimal number of components (onc) = 4 yielded quite a good fit of the experimental data with $r^2 = 0.95$ and $s = 0.200$.

The graphical representation of the model by the steric and electrostatic coefficient isocontour maps (standard deviation times coefficient) gives a clear 3-D picture of the main regions in which the electrostatic and steric interactions modulate the binding affinity. In the steric map (Fig. 1) green and red surfaces contoured regions whose occupation leads to an increase or a decrease in binding affinity, respectively. Substitution at *meta* and *para* positions seems to be sterically allowed whereas, in contrast, strong steric hindrance may be hypothe-

Table 3. Inhibition of [^{3}H]flunitrazepam binding and GABA ratio[a]

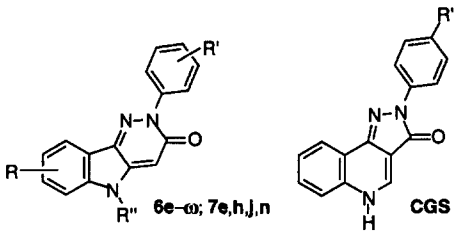

Compound	R	R′	R″	IC_{50} nM (±SD)	GABA ratio[b]
6e	H	H	H	238±18	0.94
6f	H	*p*-F	H	135±10	1.24
6g	H	*m*-F	H	95.3±7	1.45
6h	H	*p*-Cl	H	31.1±1	1.12
6i	H	*m*-Cl	H	109.6±8	1.17
6j	H	*p*-Br	H	39.4±2	1.13
6k	H	*m*-Br	H	360±48	[c]
6l	H	*o*-Br	H	[27][d]	[c]
6m	H	*p*-I	H	98±9	1.11
6n	H	*p*-OCH_3	H	23.9±1	1.02
6o	H	*p*-CH_3	H	47±1	1.50
6p	H	*m*-CH_3	H	855±79	[c]
6q	H	*o*-CH_3	H	[33][d]	[c]
6r	H	*p*-$CH(CH_3)_2$	H	992±48	[c]
6s	H	*p*-NO_2	H	26.6±4	1.08
6t[e]	H	*p*-NH_2	H	162±10	1.09
6u	7-Br	H	H	3228±472	[c]
6v	8-Br	H	H	202±10	0.78
6w	9-Br	H	H	17.5±1	1.13
6x	8-CH_3	H	H	300±51	0.85
6y	8-F	H	H	194±1	1.27
6z	8-CH_3	*p*-CH_3	H	132±7	1.10
6ω	8-F	*p*-F	H	97.1±14	0.98
7e	H	H	CH_3	1560±514	[c]
7h	H	*p*-Cl	CH_3	2485±449	[c]
7j	H	*p*-Br	CH_3	[37][d]	[c]
7n	H	*p*-OCH_3	CH_3	994±44	[c]
CGS 8216	—	H	—	1.85±0.4	N.D.[f]
CGS 9895	—	*p*-OCH_3	—	2.31±0.7	N.D.
CGS 9896	—	*p*-Cl	—	2.07±0.5	1.06
Diazepam				16.3±0.2	1.27

[a]The binding affinities and the GABA-ratios of the new ligands are reported together with those of the just described congeners **6e**, **h**, **j**, **n**.[14]
[b]GABA ratio: IC_{50} (compound)/IC_{50} (compound +20 μM-GABA).
[c]GABA ratio of low affinity compounds were not determined.
[d]Percentage of inhibition of specific [^{3}H]flunitrazepam binding at 20 μM compound concentration.
[e]Synthesized from **6s**, see Experimental.
[f]N.D.: not determined.

Table 4. Binding data and descriptors[a] used in the 2-D QSAR studies

Compound	R	R′	R″	pIC_{50}	π	π_4	MR[b]	MR_4[b]	I_N	I_m	σ	L	B_1	B_5
6e	H	H	H	6.62	0.00	0.00	0.10	0.10	0	1	0.00	2.06	1.00	1.00
6f	H	*p*-F	H	6.87	0.14	0.14	0.09	0.09	0	0	0.06	2.65	1.35	1.35
6g	H	*m*-F	H	7.02	0.14	0.00	0.09	0.10	0	1	0.34	2.65	1.35	1.35
6h	H	*p*-Cl	H	7.51	0.71	0.71	0.60	0.60	0	0	0.23	3.52	1.80	1.80
6i	H	*m*-Cl	H	6.96	0.71	0.00	0.60	0.10	0	1	0.37	3.52	1.80	1.80
6j	H	*p*-Br	H	7.40	0.86	0.86	0.89	0.89	0	0	0.23	3.82	1.95	1.95
6k	H	*m*-Br	H	6.44	0.86	0.00	0.89	0.10	0	1	0.39	3.82	1.95	1.95
6m	H	*p*-I	H	7.00	1.12	1.12	1.39	1.39	0	0	0.18	4.23	2.15	2.15
6n	H	*p*-OCH_3	H	7.62	−0.02	−0.02	0.79	0.79	0	0	−0.27	3.98	1.35	3.07
6o	H	*p*-CH_3	H	7.33	0.56	0.56	0.565	0.565	0	0	−0.17	2.87	1.52	2.04
6p	H	*m*-CH_3	H	6.07	0.56	0.00	0.565	0.10	0	1	−0.07	2.87	1.52	2.04
6r	H	*p*-$CH(CH_3)_2$	H	6.00	1.53	1.53	1.50	1.50	0	0	−0.15	4.11	1.90	3.17
6s	H	*p*-NO_2	H	7.58	−0.28	−0.28	0.74	0.74	0	0	0.78	3.44	1.70	2.44
6t	H	*p*-NH_2	H	6.79	−1.23	−1.23	0.54	0.54	0	0	−0.66	2.78	1.35	1.97
7e	H	H	CH_3	5.81	0.00	0.00	0.10	0.10	1	1	0.00	2.06	1.00	1.00
7h	H	*p*-Cl	CH_3	5.60	0.71	0.71	0.60	0.60	1	0	0.23	3.52	1.80	1.80
7j	H	*p*-Br	CH_3	4.50	0.86	0.86	0.89	0.89	1	0	0.23	3.82	1.95	1.95
7n	H	*p*-OCH_3	CH_3	6.00	−0.02	−0.02	0.79	0.79	1	0	−0.27	3.98	1.35	3.07

[a]Taken from ref. 20.
[b]Scaled by 0.1.

sized in the *ortho* and N5 regions. The green polyhedron close to position 9 seems to indicate a favourable steric region, but its definition and importance need further investigations, since only one compound substituted at position 9 is present in the present model.

In the electrostatic contour map (Fig. 2) cyan and yellow polyhedra represent zones in which an increase in negative charge is favourable or unfavourable to the binding affinity, respectively. Cyan polyhedra in the *para* region suggest favourable interactions for electron rich substituents whereas an opposite effect can be seen in the *ortho* position (yellow polyhedron). The presence of a cyan region close to the N5-methyl substituents is not easily interpretable.

Pharmacological studies

In vivo studies were performed on some selected PIs **6** and **7** to assess their pharmacological profiles as CNS active agents.

The anticonvulsant effects of PIs **6** and **7** were studied on DBA/2 mice exposed to auditory stimulation and in Swiss mice treated with the convulsant agent pentylenetetrazole (PTZ). DBA/2 is a particular strain of mice genetically susceptible to sound-induced seizures and constitutes an excellent animal model for the study of certain kinds of human epilepsy and for testing new anticonvulsant drugs.[25] The pharmacological results of our study are summarized in Table 6 along with some previous ones on other PIs **6**.

To gain insight into the mechanism of action of PI BZR ligands, it was also investigated whether the pharmacological effects of some highly active derivatives, namely **6j** and **7h**, were modified by flumazenil (a 'neutral' benzodiazepine receptor antagonist) and whether compound **6e**, a probable weak inverse agonist, was able to reduce the anticonvulsant properties of diazepam.

As far as audiogenically induced seizures are concerned, the onset of clonic and tonic seizures was significantly reduced 45 min after ip administration of derivatives **6h–j**, **n**, **o**, **s**, and **7h**. The latter, which is a N5-methylated congener, displayed the highest anticonvulsant activity, which was unexpected considering its relatively low receptor affinity. A plausible explanation may be envisaged taking into account both a more favourable diffusion across the blood brain barrier and a possible metabolic demethylation to **6h** which could be the true ligand responsible for the observed effects.

Table 5. Statistical parameters from CoMFA[a]

		n	onc	q^2	r^2	s	Ste	Ele
Alignment A (2′, 4′, 5′)		26	4	0.429	—	—	—	—
Alignment B (2′, 3′, 4′)		26	4	0.560	0.951	0.200	76	24

[a]n, number of compounds; onc, optimal number of components; r and q, correlation coefficient and cross-validated correlation coefficient, respectively; s, standard deviation; Ste and Ele, percentage of contribution to the final model of steric and electrostatic field, respectively.

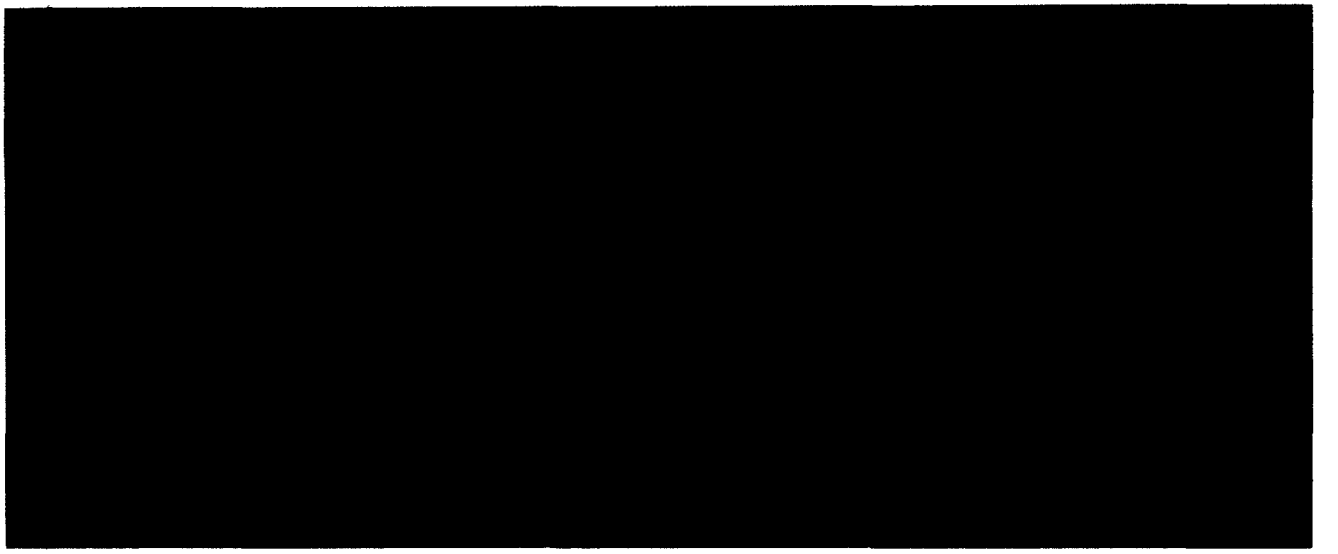

Figure 1. Stereo view of the 3-D QSAR model: steric isocontour map. The color code is as follows: favourable and unfavourable steric interactions, green and red zones, respectively. To aid interpretation compounds **6l**, **n**, **p**, **s**, **w** and **7e** have been added to the map.

The high anticonvulsant activity of **6j** and **7h** was significantly reduced by a pretreatment with flumazenil (2.5 mg/kg ip): the ED_{50} of the clonic and tonic seizures increases 2.1 and 2.78 times, respectively, for **6j**, and 3.25 and 3.67 times for **7h**.

Additional experiments showed a significant reduction in the anticonvulsant effects of diazepam upon a pretreatment with **6e**. Taken together, these findings indicate that the actions of PI derivatives can be principally mediated by interactions with BZR sites.

As shown in Table 6, the clonic and tonic seizures induced by PTZ were significantly reduced after ip administration of diazepam, **6h**, **j**, **n**, **o**, **s**, and **7h**. These effects were produced at doses higher than those observed in the audiogenic test.

The inverse agonist activity of **6v**, suggested by a GABA ratio value much lower than 1 (0.78), was fully confirmed in vivo in both assays revealing a clear proconvulsant activity of **6v** when the test was carried out at 83 dB (subconvulsant level) and at 40 mg/kg of PTZ (subconvulsant dose) (Table 6).

It is important to note that the anticonvulsant activity of the tested PIs was evident at dose levels which did not affect sedation, ataxia and in most cases body temperature. There is also some preliminary evidence that these compounds act at BZR as selective anticonvulsant and anxiolitic drugs without producing myorelaxant and sedative effects. PIs behave, therefore, as partial agonists and their effects might occur at low BZR occupation, as recently demonstrated with some benzodiazepine and β-carboline derivatives.[26-28]

Conclusions

Pyridazinoindolones **6** and **7** represent a new and interesting class of BZR ligands. 2-D QSAR studies yielded eq (1-3) that are in full agreement with previous structure-affinity relationship studies and, moreover, furnish further insight into the steric limita-

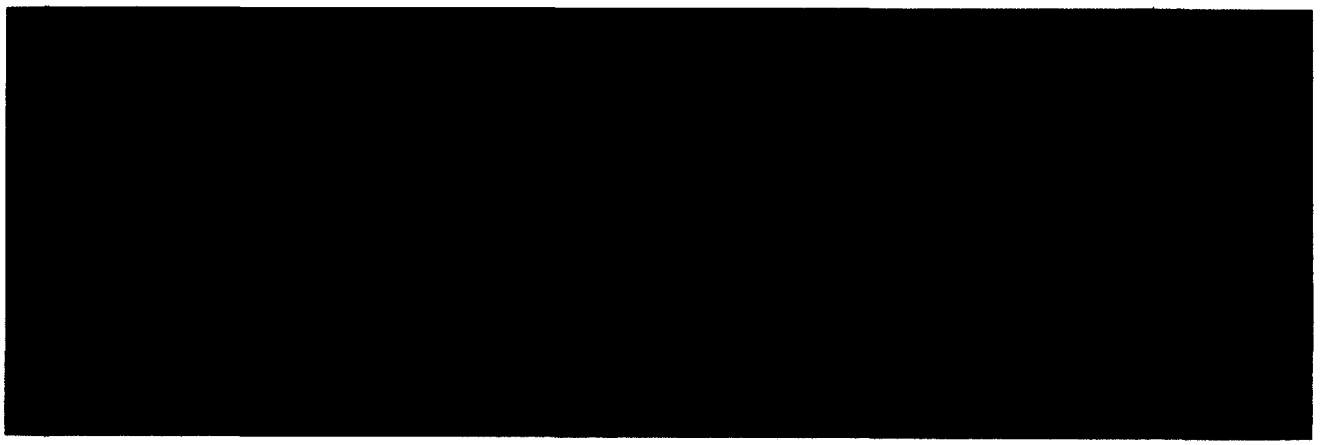

Figure 2. Stereo view of the 3-D QSAR model: electrostatic isocontour map. The color code is as follows: favourable influence of high electron density and deficiency, cyan and yellow regions, respectively. To aid interpretation, molecules **6j**, **l**, **s** and **7e** are shown in the map.

tions and complex nature of the interactions which occur at the L_2 receptor region. These points deserve additional studies which are presently in progress in our laboratory.

3-D QSAR results from CoMFA are in accordance with the 2-D QSAR analysis, supporting and complementing, at the 3-D level, some previous observations. Moreover, the present findings demonstrate that the coordinated use of 2-D and 3-D QSAR methods constitute a valuable approach to study complex biological processes, as already observed in the study of enzyme inhibition and chiral molecular recognition.[29–32]

From a pharmacological point of view, different substitution along the pyridazino-indole nucleus and the

Table 6. Pharmacological profile of compounds **6** and **7**

A. Anticonvulsant activity

Compound	R	R′	R″	Seizure phase	ED_{50}[a] (mg/kg) Inhibition of audiogenic seizures (DBA/2 mice)	ED_{50} (mg/kg) Inhibition of PTZ induced seizures (Swiss mice)
Diazepam				CLO[b]	0.08 (0.06–0.1)	0.33 (0.27–0.40)
				TON[c]	0.07 (0.04–0.1)	0.21 (0.17–0.26)
6e*	H	H	H	CLO	N.A.[d]	N.A.
				TON	N.A.	N.A.
6e + Diazepam[f]				CLO	0.21 (0.1–0.3)	N.D.[e]
				TON	0.13 (0.1–0.2)	N.D.
6h[f]	H	*p*-Cl	H	CLO	1.07 (0.5–2.2)	20.31 (10.3–39.9)
				TON	0.53 (0.2–1.2)	15.89 (6.2–40.6)
6i	H	*m*-Cl	H	CLO	14.32 (6.1–33.7)	N.D.
				TON	12.77 (6.4–25.6)	N.D.
6j[f]	H	*p*-Br	H	CLO	0.23 (0.2–0.3)	5.21 (2.4–11.4)
				TON	0.09 (0.04–0.2)	2.90 (0.9–8.7)
Flumazenil + **6j**[f]				CLO	0.48 (0.2–0.9)	N.D.
				TON	0.25 (0.1–0.4)	N.D.
6n[f]	H	*p*-OCH_3	H	CLO	0.91 (0.5–1.5)	12.70 (5.3–30.3)
				TON	0.66 (0.5–0.9)	8.49 (3.1–22.9)
6o	H	*p*-CH_3	H	CLO	0.83 (0.6–1.1)	2.21(1.36–3.59)
				TON	0.22 (0.1–0.6)	1.59(1.03–2.45)
6s	H	*p*-NO_2	H	CLO	1.45 (0.9–2.4)	3.42(1.81–6.49)
				TON	1.27 (0.7–2.3)	3.07(1.69–5.56)
6v	8-Br	H	H	CLO	N.A.	N.A.
				TON	N.A.	N.A.
7h	H	*p*-Cl	CH_3	CLO	0.08 (0.05–0.13)	3.6 (2.7–4.8)
				TON	0.06 (0.04–0.08)	2.2 (1.8–2.7)
Flumazenil + **7h**				CLO	0.26 (0.17–0.40)	N.D.
				TON	0.22 (0.15–0.32)	N.D.
CGS 9896[f]				CLO	1.13 (0.6–2.0)	57.85 (13.0–258.2)
				TON	0.83 (0.6–1.1)	13.99 (4.8–40.6)

B. Proconvulsant activity of compound **6v**

	Seizure phase	% Incidence of audiogenic seizures[g]	% Incidence of PTZ induced seizures[h]
Vehicle	CLO	10	0
	TON	0	0
6v (6.6 mg/kg)	CLO	70	60
	TON	40	40
6v (10 mg/kg)	CLO	100	80
	TON	100	60
6v (20 mg/kg)	CLO	100	100
	TON	90	90

[a]ED_{50} values with 95% confidence limits for each compound and each phase of seizure response were estimated using the Bliss method probit procedure.
[b]CLO: Clonus.
[c]TON: Tonus.
[d]N.A.: Not active.
[e]N.D.: Not detected.
[f]The activities values of compounds **6e**, **h**, **j**, **n** and CGS 9896 reported in our previous paper[14] are presented here for a better comparison of the activity data.
[g]DBA/2 mice, subconvulsant stimulus (83 dB).
[h]Swiss mice, subconvulsant dose of PTZ (40 mg/kg).

2-phenyl ring results in a complete spanning of the pharmacological activity from agonist to inverse agonist. Of particular interest was the anticonvulsant activity of compound **7h**, which in the audiogenic assay elicited an activity equal to that of diazepam. Further studies have been planned to better delineate the structure–activity relationships at the pharmacological level.

Experimental

Chemistry

Melting points were taken on a Gallenkamp MFB 595 010 M apparatus and are uncorrected. Elemental analyses were performed on a Carlo Erba 1106 analyzer; for the C, H, and N, the results agreed to within $\pm 0.40\%$ of the theoretical values. IR spectra were recorded using potassium bromide disks on a Perkin–Elmer 283 spectrophotometer, only the most significant and diagnostic absorption bands being reported. ^{1}H NMR spectra were recorded on a Bruker AM 300 WB, chemical shifts are expressed in δ (ppm) and the coupling constants J in Hz. Exchange with deuterium oxide was used to identify -OH and -NH protons. UV–vis spectra were recorded on a Hewlett-Packard P452A diode array spectrophotometer. Chromatographic separations were carried out on silica gel columns (70–230 mesh, Merck). Isatins **1a**, $\mathbf{b}_5$ (5-Br), **c** and **d** were purchased from Aldrich Chemie. Isatins $\mathbf{1b}_4$, $\mathbf{b}_6$, and $\mathbf{b}_7$ (4-Br, 6-Br, and 7-Br), not available commercially, were prepared by the method of Marvel and Hiers from the appropriate bromoanilines via the isonitrosoacetanilides.[33,34] The ring closure of *m*-substituted isonitrosoacetanilide in hot concd sulphuric acid, gave an isomeric mixture of 4- and 6-bromoisatins which were separated by fractional crystallization.[35] The preparation of **4**, **5**, **6e**, **h**, **j**, and **n** has been reported in our previous paper.[14]

2-Biscarbethoxymethylen-indolin-3-ones (3a–d). Appropriately substituted isatin **1** (68 mmol) and phosphorus (V) chloride (15 g, 81.6 mmol) were mixed with anhydrous benzene (30 mL) and refluxed for 4 h. The solution was allowed to cool to room temperature and the precipitate (imidoylchloride) was collected by filtration under dry nitrogen and washed with petroleum ether. The solid was immediately dissolved in anhydrous dioxane (100 mL) and then an equimolar solution of diethylmalonate sodium salt prepared from diethylmalonate and sodium in anhydrous dioxane (120 mL), was added dropwise. The reaction mixture was stirred at room temperature for 30 min. The sodium chloride which precipitated was filtered off, the dioxane solution was evaporated in vacuo and the residue crystallized from cyclohexane to afford the title compounds **3** in 30–50% yield.

The 7-bromo-2-biscarbethoxymethylene-indolin-3-one ($\mathbf{3b}_7$) was not synthesized because 7-bromoisatin ($\mathbf{1b}_7$) did not give the corresponding 2-chloro-3H-indol-3-one ($\mathbf{2b}_7$) as reported for the analogue 7-chloroisatin.[36]

The analytical and spectroscopic data of the novel compounds **3** are reported in Table 2. Data for **3a** have been previously described.[14]

Condensation of 3 with substituted R′-phenylhydrazines

A soln of R′-phenylhydrazine hydrochloride (2.4 mmol) in ethanol:water (1:1, 12 mL) was added to a stirred soln of **3** (2 mmol) in ethanol (40 mL) and then refluxed to give a mixture of **4** and **5** as yellow precipitates./The yields of the esters **4** and the acids **5** are reported in Table 7 together with the refluxing time.

In the case of **4–5f**, **4–5x**, **4–5z**, and **4–5o** binary mixtures, the precipitate was collected and crystallized from dioxane to obtain the carboxylic acids **5f**, **x**, and **z** or from acetonitrile to obtain **5o**. The crystallization mother liquor was then evapd in vacuo and the residue chromatographed on silica gel afforded the esters **4f**, **x**, **o** (eluent ethyl acetate:petroleum ether, 7:3, R_f 0.55; 0.56, and 0.3, respectively) and **4z** (eluent ethyl acetate:petroleum ether, 6:4, R_f 0.53).

The **4–5r** mixture was crystallized from acetic acid to give the carboxylic acid **5r**. The reaction mother liquor cooled in refrigerator for 48 h furnished the ester **4r** which was collected and crystallized from ligroin.

In the case of **4–5y** and **4–5ω** mixtures, the precipitate was first washed with chloroform and then crystallized from acetic acid to afford the carboxylic acids **5y** and **5ω**. The residue, obtained from evaporation of the chloroformic solution was crystallized from ligroin to furnish the esters **4y** and **4ω**.

The precipitates obtained from **3a** with *m*-Cl, *m*-Br, *o*-Br, *m*-CH_3, *o*-CH_3 phenylhydrazine hydrochlorides and from $\mathbf{3b}_4$ (4-Br) and $\mathbf{3b}_6$ (6-Br) with phenylhydrazine hydrochloride (1:2 molar ratio) were collected and crystallized from dioxane to give the carboxylic

Table 7. Reaction times and yields for the preparation of **4** and **5**

R	R′	Time (h)	Yields (%)	
H	*p*-F	8	**4f** (42)	**5f** (17)
H	*m*-F	1	**4g** (50)	
H	*m*-Cl	6	**4i** (18)	**5i** (22)
H	*m*-Br	12	**4k** (25)	**5k** (46)
H	*o*-Br	6	**4l** (10)	**5l** (15)
H	*p*-I	8	**4m** (20)	**5m** (40)
H	*p*-CH_3	8	**4o** (23)	**5o** (15)
H	*m*-CH_3	10	**4p** (29)	**5p** (39)
H	*o*-CH_3	10	**4q** (30)	**5q** (40)
H	*p*-$CH(CH_3)_2$	8	**4r** (23)	**5r** (56)
H	*p*-NO_2	3	**4s** (33)	**5s** (29)
7-Br	H	5	**4u** (43)	**5u** (10)
8-Br	H	12	**4v** (72)	**5v** (15)
9-Br	H	8	**4w** (20)	**5w** (10)
8-CH_3	H	7	**4x** (59)	**5x** (14)
8-F	H	4	**4y** (44)	**5y** (11)
8-CH_3	*p*-CH_3	7	**4z** (59)	**5z** (11)
8-F	*p*-F	3	**4ω** (26)	**5ω** (5)

acids **5i, k, l, p, q, w,** and **u**, respectively. The residue obtained upon evaporation of the reaction mother liquors was crystallized from ligroin to furnish the esters **4i, k, l, p, q,** and **u**, respectively, or chromatographed on silica gel to give ester **4w** (eluent chloroform:ethyl acetate, 8:2, R_f 0.50).

Compounds **4m** and **5m** were obtained by refluxing **3a** with *p*-iodophenylhydrazine and an equimolar amount of conc HCl in ethanol/water. Upon cooling first at room temperature and then in the refrigerator **5m** and **4m** were obtained, respectively.

Compounds **4s** and **5s** were obtained from **3a** by reaction with *p*-nitrophenylhydrazine and an excess of conc HCl. The yellow precipitate was worked up as described for **4–5y** mixture to give the carboxylic acid **5s** and the ester **4s** (eluent chloroform:ethylacetate, 85:15, R_f 0.43).

The reactions of **3a** with an equimolar amount of *m*-fluorophenylhydrazine hydrochloride and of $\mathbf{3b_5}$ (5-Br) with an excess of unsubstituted phenylhydrazine hydrochloride (1:3) gave only the ester **4g** and **v**, respectively, which were collected and crystallized from ligroin.

Further reflux of the reaction mother liquors only in the case of $\mathbf{3b_5}$ (5-Br) furnished the carboxylic acid **5v**.

Hydrolysis of esters 4

A soln of NaOH (0.200 g, 5 mmol) in ethanol (15 mL) was added to a stirred suspension of **4** (0.5 mmol) in ethanol (7.5 mL) and then refluxed for 1 h. The reaction mixture was cooled to room temperature and the solvent evapd in vacuo. The aqueous (60 mL) suspension of the residue was acidified with conc HCl to pH 1 and stirred at room temperature for 2 h. The yellow solid was filtered, washed with water, and dried. Crystallization (see Table 2) gave pure carboxylic acids **5** in 85–90% yield.

Thermal decarboxylation of 5

A sealed glass tube containing the acids **5** (0.3 mmol) was heated at 320–360 °C for 5–9 min (Table 7). After cooling to room temperature, the solid was chromatographed on silica gel using ethyl acetate:methanol (9:1) as eluent to give compounds **6**. R_f values and yields are reported in Table 8.

2-*p*-Aminophenyl-2,5-dihydropyridazino[4,3-*b*] indol-3(3H)-one (6t). A mixture of **6s** (30.6 mg, 0.1 mmol) in dioxane (15 mL) and 10% Pd/C (15 mg) was shaken with hydrogen at 50 psi for 4 h. The catalyst was then filtered off and the filtrate evapd in vacuo. The residue was chromatographed on silica gel using ethyl acetate: methanol, 9:1 as eluent, to yield compound **6t** (12 mg, 43% yield, R_f 0.35).

2-Aryl-5-methyl-2,5-dihydropyridazino[4,3-*b*]indol-3(3H)-ones (7e, h, j, and n). Sodium hydride (97%, 10 mg, 0.40 mmol) was added to a stirred suspension of **6** (0.19 mmol) in dry tetrahydrofuran (1.5 mL) at room temperature, under nitrogen. Stirring was continued for 40 min and iodomethane (99%, 25 μL, 0.40 mmol) was added. After 2 h, the yellow precipitate was filtered and washed with ether to give the crude compound **7**.

Table 8. Experimental conditions for thermal decarboxylation of **5** to **6**

Compound	Temp. °C	Time (min)	R_f[a]	Yield %
6f	350	5	0.48	86
6g	320	8	0.73	50
6i	325	7	0.71	72
6k	320	6	0.79	62
6l	320	6	0.63	56
6m	335	5	0.62	70
6o	330	6	0.47	76
6p	325	7	0.73	76
6q	320	8	0.73	70
6r	330	5	0.52	79
6s	330	7	0.62	61
6u	350	5	0.74	62
6v	360	5	0.50	59
6w	350	9	0.64	90
6x	320	7	0.60	30
6y	320	5	0.54	73
6z	325	7	0.75	30
6ω	340	5	0.70	76

[a]See Experimental for the eluents.

Compounds **7e** and **n** were purified by crystallization from methanol in 55 and 54% yield, respectively. Compound **7j** was purified by crystallization from dioxane (48 mg, 68% yield). Compound **7h** was first chromatographed on silica gel (chloroform:methanol, 9:1 as eluent) and then crystallized from methanol (39 mg, 66% yield, R_f 0.61).

2-D QSAR study

Correlation analysis. A multiple regression analysis was performed by means of the software QSAR of Hoeckman-Hansch-Leo (Pomona College, Claremont, CA, U.S.A.). The binding data and the substituent constants used in the present study are listed in Table 4. The electronic and hydrophobic effects of substituents were assessed by the classical Hammett and Hansch substituent constants, σ and π, respectively. The molar refractivity MR and the STERIMOL Verloop parameters L, B_1, and B_5 were employed to model bulkiness and polarizability effects. The σ, π, MR, L, B_1, and B_5 values were taken from standard compilations.[20]

3-D QSAR Studies

Molecular modelling. Computational approaches. All the theoretical and modelling studies were performed on a Silicon Graphics Indigo 2 workstation using the SYBYL 6.1 molecular modelling software (Tripos, St. Louis, MO, U.S.A.).

Conformational analysis and alignment. All the compounds were built from fragments of the SYBYL library and fully optimized by the AM1 Hamiltonian. Partial atomic charges were from AM1 calculations.

The conformational analysis was carried out with the systematic search protocol on the inter ring rotatable bond $C_3N_2C_1{\cdot}C_2{\cdot}$ from 0 to 360° (0–180° for substitution) in 30° increments.

The conformers selected for the different alignments had a torsion angle of −74° and an energy content comprised within 1 kcal/mol above the absolute energy minimum. The torsion angle of −74° corresponds to a mean value of the minimum energy conformers for the *ortho* substituted congeners.

The selected conformers were aligned by superimposing all the atoms of the common condensed tricyclic system by the MULTIFIT procedure of SYBYL.

CoMFA interaction energy calculations. For each alignment set, the steric (6/12 Lennard–Jones) and electrostatic (Coulomb) potential energy fields were calculated at each lattice intersection on a regularly spaced grid of 2 Å.

An sp^3 carbon atom with a van der Waals radius of 1.52 Å and a +1 charge was used as the probe to calculate the steric and electrostatic fields.

Partial least squares (PLS) analysis. To derive 3-D QSAR models, the method of partial least squares (PLS) fitting was used. A PLS run was initially applied with cross-validation to determine the optimal number of components (onc) needed for the subsequent analysis providing the final non cross-validated 3-D QSAR model which was used to draw the coefficient contour maps in Figures 1 and 2. The onc was chosen as that yielding the largest cross-validated r^2 (q^2). q^2 is defined as follows: (SD-PRESS)/SD where SD is the sum of squares of deviations of the observed values from their mean and PRESS is the prediction sum of squares. q^2 gives an estimation of the predictive ability of the model. CoMFA default settings were used throughout the study.

Binding and pharmacological studies. The binding affinities and the pharmacological data, reported in Tables 3 and 6, respectively, were obtained by the methods previously described by us.[14]

Acknowledgements

The authors are grateful to CNR (Rome) and MURST (Rome) for financial support. The skillful assistance of Dr M.L. Barreca in molecular modelling and of Mr Anthony Green in reviewing the English is gratefully acknowledged.

References

1. Kerr, I. B.; Ong, J. *Med. Res. Rev.* **1992**, *12*, 593.

2. *GABA and Benzodiazepine Receptors*; Squires R., Ed.; CRC: Boca Raton; 1988; Vols 1–2.

3. Bernard, E. A. In *$GABA_A$ Receptor and Anxiety. From Neurobiology to Treatment*; Biggio, G.; Sanna, E.; Costa, E., Eds., Raven: New York, 1995; pp 1–16.

4. Smith, G. B.; Olsen, W. R. *Trends Pharmac. Sci.* **1995**, *16*, 162.

5. De Lorey, T. M.; Olsen, R. W. *J. Biol. Chem.* **1992**, *262*, 6747.

6. Tulinsky, J.; Gammill, L. B. *Curr. Med. Chem.* **1994**, *3*, 226.

7. Lader, M. In *$GABA_A$ Receptor and Anxiety. From Neurobiology to Treatment*; Biggio, G.; Sanna, E.; Costa, E., Eds., Raven: New York, 1995; pp 135–152.

8. Allen, M. S.; Tan, Y. C.; Trudell, M. L.; Schindler, L. R.; Martin, M. J.; Schulz, C.; Hagen, T. J.; Koehler, K. F.; Codding, P. W.; Skolnick, P.; Cook, J. M. *J. Med. Chem.* **1990**, *33*, 2343.

9. Villar, H. O.; Davies, M. F.; Loew, G. H.; Maguire, P. A. *Life Sci.* **1991**, *48*, 593.

10. Diaz–Arauzo, H.; Koehler, K. F.; Hagen, T. J.; Cook, J. M. *Life Sci.* **1991**, *49*, 207.

11. Allen, M. S.; Skolnick, P.; Cook, J. M. *J. Med. Chem.* **1992**, *35*, 368.

12. Schove, L. T.; Perez, J. J.; Loew, G. H. *Bioorg. Med. Chem.* **1994**, *2*, 1029.

13. Zhang, F.; Koehler, K. F.; Zhang, P.; Cook, J. M. *Drug Des. Dis.* **1995**, *12*, 193.

14. Campagna, F.; Carotti, A.; Casini, G.; Palluotto, F.; Genchi, G.; De Sarro, G. B. *Bioorg. Med. Chem.* **1993**, *1*, 437.

15. Trofimov, F. A.; Garnova, V. I.; Tshskova N. G. *Kim. Geterotsikl. Soedin.* **1985**, *5*, 640.

16. Fryer, R. I.; Zhang, P.; Rios, R.; Gu, Z.-Q.; Basile, A. G.; Skolnick, P. *J. Med. Chem.* **1993**, *36*, 1669.

17. Hansch, C.; Leo, A. In *Exploring QSAR*; ACS: Washington, 1995; Vol. 1.

18. Cramer, R. D.; Patterson, D. E.; Bunce, J. D. *J. Am. Chem. Soc.* **1988**, *110*, 5959.

19. *3D-QSAR in Drug Design*; Kubiniy, H., Ed.; Escom: Leiden, 1993.

20. Hansch, C.; Leo, A.; Hoeckman, D. In *Exploring QSAR*; ACS: Washington, 1995; Vol. 2.

21. Selassie, C. D.; Klein, T. E. In *3D-QSAR in Drug Design*; Kubiniy, H., Ed.; Escom: Leiden, 1993; pp 257–275.

22. Carotti, A.; Hansch, C.; Mueller, M. M.; Blaney, J. M. *J. Med. Chem.* **1984**, *27*, 1401.

23. Carotti, A.; Raguseo, C.; Klein, T. E.; Langridge, R.; Hansch, C. *Chem. Biol. Int.* **1988**, *67*, 171.

24. Carrieri, A.; Altomare, C.; Barreca, M. L.; Contento, A.; Carotti, A.; Hansch, C. *Il Farmaco* **1994**, *49*, 573.

25. Trichlebank, M. D.; Honore, T.; Iversen, S. D.; Kemp, J. A.; Knight, A. R.; Marshall, G. R.; Rupniak, N. M. J.; Singh, L.; Tye, S.; Watjen, F.; Wong, E. H. F. *Br. J. Pharmacol.* **1990**, *101*, 753.

26. Duka, T.; Hoellt, V.; Hertz, A. *Brain Res.* **1979**, 147.

27. Jensen, L. H.; Petersen, E. N.; Braestrup, C. *Life Sci.* **1983**, *33*, 393.

28. De Sarro, G. B.; Zappalà, M.; Grasso, S.; Chimirri, A.; De Sarro, A. *Gen. Pharmacol.* **1993**, *24*, 877.

29. Thull, U.; Altomare, C.; Carta, V.; Paillard, P.; Carrupt, P.; Carotti, A.; Testa, B. *J. Med. Chem.* **1995**, *38*, 3874.

30. Thull, U.; Kneubuhler, S.; Gaillard, P.; Carrupt, P.; Testa, B.; Altomare, C.; Carotti, A.; Jenner, P.; McNaught, K. St. P. *Biochem. Pharmacol.* **1995**, *50*, 869.

31. Carotti, A.; Altomare, C.; Cellamare, S.; Monforte, A. M.; Bettoni, G.; Loiodice, F.; Tangari, N.; Tortorella, V. *J. Comp.-Aid.Mol.Des.* **1995**, *9*, 131.

32. Altomare, C.; Carotti, A.; Cellamare, S.; Fanelli, F.; Gasparrini, F.; Villani, C.; Carrupt, P.-A.; Testa, B. *Chirality* **1993**, *5*, 527.

33. Marvel, C. S.; Hiers, G. S. *Organic Synthesis, Coll.* 1941, *Vol. 1, 2nd ed.* p. 327.

34. Sandmeyer, T. *Helv. Chim. Acta* **1919**, *2*, 234.

35. Sadler, P. W. *J. Org. Chem.* **1956**, *21*, 169.

36. Grimshaw, J.; Begley, J. W. *Synthesis* **1974**, 497.

(*Received in U.S.A.* 11 *June* 1996; *accepted* 2 *August* 1996)